

## Interaction of a rectangular jet with a slotted plate in presence of a control mechanism: Experimental study of the aeroacoustic field

Marwan Alkheir<sup>1,a\*</sup>, Hassan Assoum<sup>2</sup>, Nour Eldin Afyouni<sup>1,b\*</sup>, Bilal El Zohbi<sup>1</sup>,  
Kamel Abed Meraim<sup>1</sup>, Anas Sakout<sup>1</sup>, Mouhammad El Hassan<sup>3,c\*</sup>

<sup>1</sup> LASIE UMR CNRS 7356, University of La Rochelle, La Rochelle, France

<sup>2</sup> Beirut Arab University, Mechanical Engineering Department, Tripoli, Lebanon

<sup>3</sup> Prince Mohammad Bin Fahd University, Mechanical Engineering Department, Al Khobar, KSA

<sup>a</sup> marwanalkheir@gmail.com, <sup>b</sup> nour.afyouni@gmail.com, <sup>c</sup> melhassan@pmu.edu.sa

**Keywords:** Aeroacoustics, Rectangular Jet, SPIV, Passive Control, Acoustic Comfort, Fluid-Structure Interaction

**Abstract.** The acoustic comfort inside residential buildings is of high interest. HVAC systems employ different shapes of diffusers to ensure air mixing. The interaction between the airflows and the blades of these terminals may result in intense noise radiation. In this work, an experimental study was carried out to investigate the aero-acoustic production of a rectangular jet impinging on a rectangular plate with a slot. For certain flow regimes, such configuration results in whistles with high acoustic levels, called "self-sustaining tones". These tones result from the interaction between the Aerodynamic modes of the jet and acoustic modes. The impact of the vortical structures on the rectangular plate results in pressure waves that re-excite the jet near its exit. This feedback mechanism and the aero-acoustic coupling are responsible for the high-energy tones and can lead to structural fatigue through vibrations. A control mechanism consisting of a thin rod was introduced between the jet nozzle and the impinging wall to disturb the vortex dynamics responsible for the loop of the self-sustaining tones. A total of 1085 positions of the rod were tested between the nozzle and the impinged plate to identify positions of optimal noise reduction. Simultaneous Stereoscopic Particle Image Velocimetry (SPIV) and unsteady pressure measurements were conducted to characterize both the kinematic and the acoustic fields. Two zones were distinguished in terms of control efficacy. In the first one, the sound pressure level dropped by 19 dB, while in the second zone, the sound pressure level increased by 14 dB. The velocity fields show that the presence of the rod divides the main jet into two lateral jets from both sides of the axis of the convergent. The presence of the cylinder creates an artificial expansion of the jet and divides it into two shear flows or jet-like flows. The outer part of these flows expands radially with less interaction with the plate as compared to the case without control. This behavior affects the deformation of vortices against the slot and results in a disappearance of the loop of self-sustaining tones. The main novelty of this work relates to the implementation and analysis of a control mechanism using 2D3C (SPIV) velocity measurements simultaneously with the acoustic radiation produced by the interaction of this flow with a slotted impinging wall.

### Introduction

Impinging jets received great interest for several industrial applications; they are used in cooling of electronic parts, in building HVAC systems, in drilling process, and various other applications. The interaction of a jet with a solid surface may, in certain configurations listed by [1], generates whistles with a considerable acoustic level, which are called "Self-sustaining tones". The self-sustaining tones have been studied by [1]–[3]: When a turbulent jet impacts a solid surface, the surface pressure fluctuations create a periodic wave with a fundamental frequency  $f_0$ . The wave's oscillations pass upstream towards the nozzle, disturb the shear layer, and interact with the formed

structures at the jet exit. These oscillations are called feedback loops. Several studies focused on the impinging jet noise in different configurations, such as the hole tone [4], an airflow around a cylinder [5], the slot tone [6]–[10], and others. The understanding of the source of noise in impinging jet is of high importance to develop a control mechanism that would lead to reducing the sound level in these jets. Two types of control methods are presented: Passive and Active control. When compared to active control, the passive control doesn't require external energy source, such as changing the jet geometry. [11] studied the noise reduction of a twin jet nozzle using flexible filaments; they demonstrated that the filaments consistently eliminated screech tones and reduced overall sound pressure level by 3 dB or more depending on the configuration. Using circular cylinders with soft porous cover in the flow was also used to reduce jet noise. [12] studied the materials of the porous cover experimentally and found that the use of low airflow resistivity materials leads to a noticeable flow noise reduction. Circular cylinders were also used to reduce noise generated by rectangular cavities that are characterized by similar Aero-Acoustic coupling found in rectangular jets [13], [14]. For active flow control, [15] placed a circular array of 400  $\mu\text{m}$  diameter supersonic microjets around the periphery of the main jet, which reduced the near-field noise by about 8 dB. A similar method was proposed by [16] who suggested two control strategies using microjets: the first method consisted of a steady microjet injection, while the second was based on a pulsed microjet injection, motivated by the need to further improve the noise suppression. The authors found that the pulsed microjet was able to bring about the same noise reduction as a steady injection using approximately 40% of the corresponding mass flow rate of the steady microjet case. [17] studied experimentally how plasma actuators based on surface barrier high-frequency discharge affect jet noise characteristics. They showed that jet excitation in the case of  $St \approx 0.5$  using the barrier discharge plasma actuator leads to broadband amplification of jet sound radiation. The jet excitation in the case of  $St > 2$  led to broadband noise reduction if the action is sufficiently intensive.

In this paper, a passive control mechanism comprising a 4 mm diameter rod installed in the flow to disturb the vortex dynamics responsible for the loop of self-sustaining tones installed along the jet is studied experimentally using acoustic measurements and SPIV technique. The configuration consists of a rectangular air jet impinging on a slotted plate, with an impact ratio  $L/H = 4$ , where  $L$  is the distance between the plate and the nozzle distance, and  $H$  is the height of the slot. This configuration corresponds to a flow producing self-sustaining tones. In the present study, a Reynolds number  $Re = 6700$  is considered. This Reynolds number corresponds to a flow regime with a significantly high acoustic level. In order to find the optimal position of the rod, the distance between the jet outlet and the slotted plate was swept with a step of 1 mm along the  $X$  and  $Y$  axes, thus a total of 1085 rod positions were tested. An innovative technique that called Combined Stereoscopic PIV (C-SPIV) was used to resolve some experimental difficulties caused by the introduction of the rod in the flow. A detailed explanation of this technique is present in [18].

### Experimental Setup and Metrology

The experimental device (shown in Fig. 1) consists of a compressor located outside of the experimental chamber. This compressor is controlled by a chopper frequency (Siemens MICROMASTER 420, three-phases) which allow us to vary the outlet velocity from 0  $m/s$  up to 33  $m/s$  ( $M \approx 0.1$ ). The pulsed air passes through a large enclosure ( $V = 1 \text{ m}^3$ ) equipped with grids before the airflow is ejected into the flow duct of 1250  $mm$  length, with a rectangular section of dimensions 190  $mm \times 90 \text{ mm}$ . The latter contains honeycombs to parallelize the air streamlines before it arrives at a 4<sup>th</sup>-degree polynomial convergent form, of exit height  $H = 10 \text{ mm}$  and width  $Lz = 190 \text{ mm}$ . The jet coming out of the convergent will strike a slotted aluminum plate with 4  $mm$  thickness and 250  $mm \times 250 \text{ mm}$  section. This plate has a slot of the same size as the jet outlet ( $H = 10 \text{ mm}$ ,  $Lz = 190 \text{ mm}$ ). The slot is beveled at 45° downstream and aligned with the

blowing mouth. The impact distance  $L$  between the jet outlet and the plate is taken equal to 4 times the nozzle height. Thus, the dimensionless distance  $L/H = 4$  will be used in this study. To study the influence of the rod positions on the noise emission, specific fixing and displacement systems are needed to control the position of the rod. Following a control program developed in "LabVIEW", the rod can move in the x and y directions; in the x-direction, the rod can move from  $X = -15\text{mm}$  (below the jet) to  $X = 15\text{mm}$  (above the jet), however, in the y-direction, the rod starts at  $Y = 3\text{mm}$  (where the rod has a radius of  $2\text{ mm}$  with an initial safety distance of  $1\text{ mm}$ ) and moves up to the border of the split plate at position  $Y = 37\text{ mm}$  (we leave  $2\text{ mm}$  radius of the rod and  $1\text{ mm}$  of safety). Then, the rod occupies the horizontal positions  $-15\text{ mm} \leq X \leq 15\text{ mm}$  and  $3\text{ mm} \leq Y \leq 37\text{ mm}$  to fit a total of 1085 positions. For the acoustic measurements, a microphone B&K of type 4189 was placed at a  $15\text{ cm}$  distance behind the plate. We carried out our acoustic measurements with a sampling frequency of  $15\text{ kHz}$ , for 3 seconds. These acoustic signals were acquired by LabVIEW software installed on a National Instruments *NI PXI 1036* workstation equipped with a dynamic card *NI PXI 4496*. A spectral analysis is then performed in order to understand the effect of the rod on the frequency activities. To correlate the acoustic behavior to the turbulent activity, the vortex structures are identified using the Combined Stereoscopic Particle Image Velocimetry technique (C-SPIV). To seed the flow, olive oil was used as tracers, using an oil particle generator that has an oil-air atomizer sprayed by a "Laskin Nozzle" aerographic system marketed by "Lavision". For the lighting system, Litron *Nd: YLF LDY 304-PIV* laser having two heads of  $30\text{ mJ/pulse}$  at a frequency of  $1\text{ KHz}$  and a wavelength  $\lambda = 527\text{ nm}$  is used (shown in Fig. 1). The laser light beam is carried by a laser arm to illuminate the area between the jet nozzle and the plate. This laser arm contains 7 mirrors capable to transmit 96% of the light intensity. This beam is transformed into a laser sheet by a sheet generator. Thus, the thickness of the laser sheet and its opening angle is adjusted depending on the used divergent lens with a focal length of  $10\text{ mm}$ , which is chosen to withstand the high light power generated by the laser. Once the laser sheet has been generated between the nozzle and the slotted plate, images can be acquired. The synchronization between the laser pulses and the camera apertures is controlled by a high-speed controller (HSC) from "Lavision".

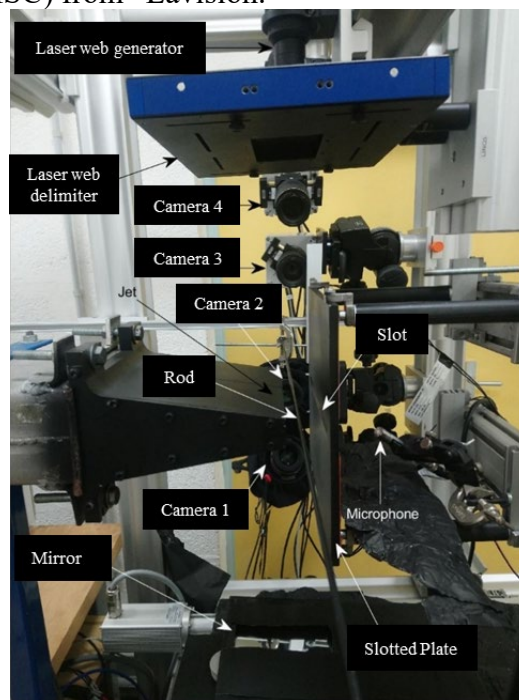
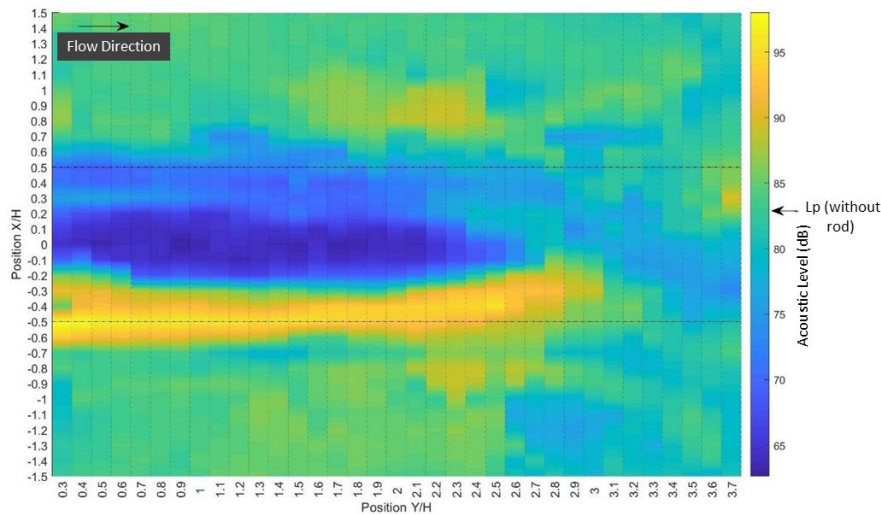


Fig. 1: Experimental setup consisting of a rectangular nozzle, slotted plate, PIV systems and Microphones

## Results and Discussion

The distribution of the sound pressure levels as a function of rod positions is shown in Fig. 2. This figure shows the results of the acoustic pressure measurements for 1085 positions occupied by the rod. It shows the influence of flow disturbance introduced by the rod on the radiated sound field. For Reynolds number  $Re = 6700$  with an impact ratio  $L/H = 4$ , in the absence of the rod, the sound pressure level produced by the self-sustaining sound is  $Lp = 83 \text{ dB}$ . The analysis of results indicates the presence of three different zones: The first zone (blue color) where the flow disturbance generated by the presence of the rod cause a reduction in the sound pressure level  $Lp$ , which can reach up to  $19 \text{ dB}$ . This area has the height of the nozzle and is located on either side of the axis of symmetry of the jet. This symmetry degrades from a longitudinal distance  $H$  from the outlet of the nozzle. However, the efficiency remains significant up to a distance of  $26 \text{ mm}$  from the jet exit. The second zone (orange and yellow color) corresponds to an increase in the sound field, which can reach up to  $+14 \text{ dB}$ . This zone is not symmetrical with respect to the axis of the jet, it occupies longitudinally ( $y$  axis) about  $28 \text{ mm}$  from the jet's outlet and the vertical positions ( $x$  axis) are approximately between  $-0.65 < X/H < -0.45$ . It can be noted that this zone gradually extends in a non-symmetrical way from the longitudinal position  $Y/H = 1.5$  to  $Y/H = 3$ . One can also notice a small zone at the level of the plate which represents a small rather significant increase in the level of the acoustic field. The third zone, apart from zones 1 and 2, where the rod does not disturb the radiated acoustic field. In this zone the acoustic level frequency characteristics are the same as those found in the absence of the rod.

To understand the effect of the rod on the flow dynamics as well as the noise production, the acoustic and PIV data are considered simultaneously. A Fast Fourier Transform is applied on the acoustic signal to find the frequency of the sound emission. Fig. 3 shows the acoustic spectrum with and without the rod. Two positions of the rod were chosen: ( $X/H = 0$ ,  $Y/H=0.8$ ) and ( $X/H = -0.5$ ,  $Y/H=0.4$ ), which correspond to arbitrary points in zone 1 and zone 2, respectively. It is found that the presence of the rod in these positions is accompanied with a reduction of  $19,3 \text{ dB}$  and an increasing of  $8,6 \text{ dB}$  respectively. The spectrum shows that, when there was no rod in the flow, the acoustic spectrum presents three energetic frequencies:  $168 \text{ Hz}$ ,  $212 \text{ Hz}$ , and  $380 \text{ Hz}$ . However, when the rod is installed at the first position, one can noticed the total disappearance of the peaks corresponding to the frequencies  $168 \text{ Hz}$  and  $320 \text{ Hz}$  which characterize the two self-sustaining sound loops in the absence of the rod. One can also observe that the frequency activity is reduced and the broadband spectrum is very weak for this rod position. This explains the dramatic reduction in the sound pressure level of  $19.3 \text{ dB}$ . When the rod occupies the second position, the spectrum indicates the disappearance of the self-sustaining sound loops. In addition, it has a broadband appearance with high-frequency activity, which explains the  $8.6 \text{ dB}$  increase in sound pressure level. One can also notice the absence of any particular frequency peaks.



*Fig. 2: Variation of the sound level as a function of the position of the rod for a Reynolds number  $Re = 6700$ , an impact ratio  $L/H = 4$  and for a rod of 4 mm*

In order to understand the origin of the variation in the acoustic spectrum, the  $\lambda_2$  criteria are calculated from the velocity field obtained by SPIV measurement. Fig. 4a shows that, when the rod occupies the position 1, the rod divides symmetrically the main jet on two jets: upper jet (in the positive y side) and lower jet (in negative y side). The two jets present an antisymmetric character dominating the vortex organization. Moreover, one note that the vortex structures coming from the upper and the lower jet strike the wall of the plate, with a strong vortex activity creating two zones of recirculation on either side of the slot, without passing through. This explains the disappearing of the frequency activity in the acoustic spectrum. However, when the rod occupies the second position (Fig. 4b), the lower jet shows no vortex activity, however the flow of the upper jet presents an antisymmetric character and the presence of the rod delays the formation of vortex structures. The coherent structures developed in the lower part of the upper jet pass completely through the slot, without interaction with the slot edge. This passage does not create feedback loop, and then no self-sustaining tones are created, which explain the disappearance of the energetic frequency in the acoustic spectrum.



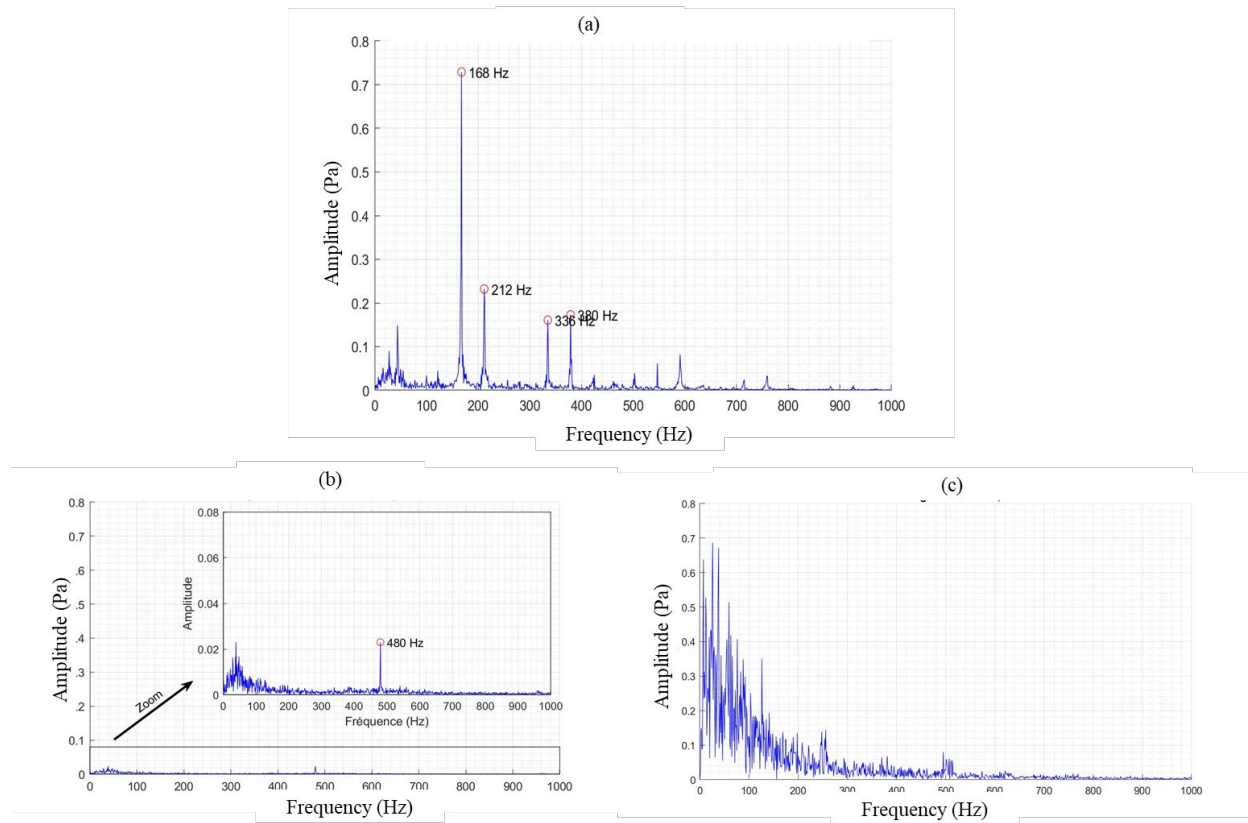


Fig. 3: Acoustic Pressure Spectra (a) in the absence of the rod, (b) in the presence of the rod at position 1: ( $X/H = 0$ ,  $Y/H=0.8$ ), (c) in the presence of the rod at position 2: ( $X/H= -0.5$ ,  $Y/H=0.4$ )

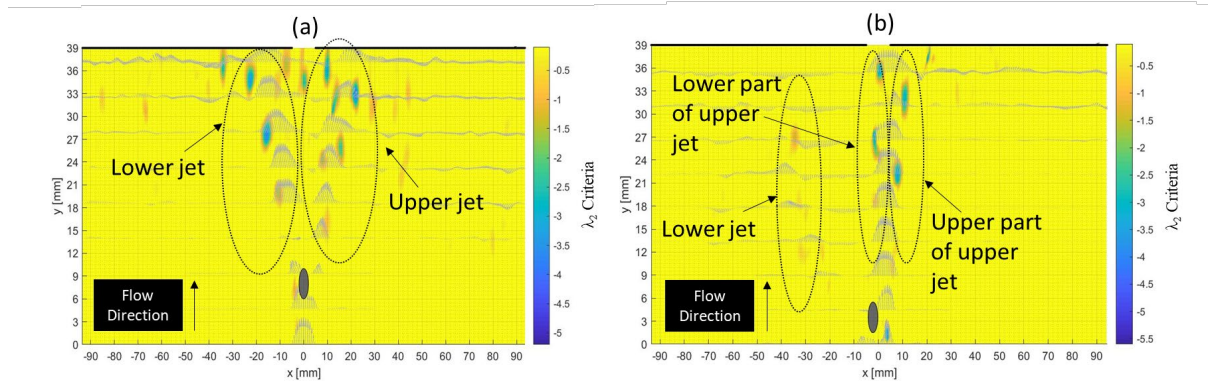


Fig. 4: The  $\lambda_2$  criteria (a) in the presence of the rod at ( $X/H = 0$ ,  $Y/H=0.8$ ), (b) in the presence of the rod at ( $X/H= -0.5$ ,  $Y/H=0.4$ )

### Conclusion

In this paper, the correlations between the vortex dynamics and the radiated sound fields are investigated experimentally using Combined Stereoscopic PIV and acoustic measurements. The analyzed flow is characterized by Reynolds number of  $Re = 6700$  with an impact ratio  $L/H = 4$ . The flow control consisted of positioning a rod of 4 mm diameter in the free jet part of the impinging jet. Two zones are distinguished: Zone 1, in which the presence of the rod leads to decreasing the sound level, and zone 2, in which the presence of the rod increases the sound level. In Zone 1, the presence of the rod causes the disappearance of self-sustaining sound loops and a low-frequency activity that characterizes the broadband spectrum appeared. It was also found that

the rod splits the flow into two jets which settle in the upper and lower part of the flow, respectively. These two jets are almost symmetrical about the main axis of the jet. In addition, in this configuration, the rod totally destabilized the flow, and lead to destroying the self-sustaining sound loops that were installed when there was no control device within the flow. In zone 2, the results show that, the presence of the rod causes the disappearance of the self-sustaining sound loops, and the appearance of a broadband spectrum with high-frequency activity, despite an increase in the sound pressure level. Dynamically, the presence of the rod divided the flow into two streams. The activity of the vortex structures resulting from the upper jet is antisymmetric, while the lower jet shows no vortex activity.

## References

- [1] D. Rockwell and E. Naudascher, "Self-Sustained Oscillations of Impinging Free Shear Layers," *Annu. Rev. Fluid Mech.*, vol. 11, no. 1, pp. 67–94, Jan. 1979. <https://doi.org/10.1146/annurev.fl.11.010179.000435>
- [2] A. Powell, "On the Mechanism of Choked Jet Noise," *Proc. Phys. Soc. Sect. B*, vol. 66, no. 12, pp. 1039–1056, Dec. 1953. <https://doi.org/10.1088/0370-1301/66/12/306>
- [3] C.-M. Ho and N. S. Nosseir, "Dynamics of an impinging jet. Part 1. The feedback phenomenon," *J. Fluid Mech.*, vol. 105, no. 1, p. 119, Apr. 1981. <https://doi.org/10.1017/S0022112081003133>
- [4] R. C. Chanaud and A. Powell, "Some Experiments concerning the Hole and Ring Tone," *J. Acoust. Soc. Am.*, vol. 37, no. 5, pp. 902–911, May 1965. <https://doi.org/10.1121/1.1909476>
- [5] A. Henning, K. Kaepernick, K. Ehrenfried, L. Koop, and A. Dillmann, "Investigation of aeroacoustic noise generation by simultaneous particle image velocimetry and microphone measurements," *Exp. Fluids*, vol. 45, no. 6, pp. 1073–1085, Dec. 2008. <https://doi.org/10.1007/s00348-008-0528-y>
- [6] K. Abed-Meraïm, H. Assoum, and A. Sakout, "TRANSFERTS ENERGETIQUES ENTRE LE CHAMP TURBULENT D'UN JET IMPACTANT DE VENTILATION ET LE CHAMP ACOUSTIQUE GENERE," 2016.
- [7] H. H. Assoum, J. Hamdi, K. Abed-Meraïm, M. El Hassan, A. Hammoud, and A. Sakout, "Experimental investigation the turbulent kinetic energy and the acoustic field in a rectangular jet impinging a slotted plate," *Energy Procedia*, vol. 139, pp. 398–403, Dec. 2017. <https://doi.org/10.1016/j.egypro.2017.11.228>
- [8] J. Hamdi, H. Assoum, K. Abed-Meraïm, and A. Sakout, "Analysis of the effect of the 3C kinematic field of a confined impinging jet on a slotted plate by stereoscopic PIV," *Eur. J. Mech. - BFluids*, vol. 76, pp. 243–258, Jul. 2019. <https://doi.org/10.1016/j.euromechflu.2019.02.012>
- [9] H. H. Assoum, M. El Hassan, J. Hamdi, M. Alkheir, K. A. Meraim, and A. Sakout, "Turbulent Kinetic Energy and self-sustaining tones in an impinging jet using High Speed 3D Tomographic-PIV," *Energy Rep.*, vol. 6, pp. 802–806, Feb. 2020. <https://doi.org/10.1016/j.egypro.2019.12.018>
- [10] H. H. Assoum *et al.*, "Turbulent kinetic energy and self-sustaining tones: Experimental study of a rectangular impinging jet using high Speed 3D tomographic Particle Image Velocimetry," *J. Mech. Eng. Sci.*, vol. 14, no. 1, pp. 6322–6333, Mar. 2020. <https://doi.org/10.15282/jmes.14.1.2020.10.0495>
- [11] N. Lucas, M. Doty, L. Taubert, and I. Wagnanski, "Reducing the noise emanating from a twin jet nozzle using flexible filaments," *Exp. Fluids*, vol. 54, no. 4, p. 1504, Apr. 2013. <https://doi.org/10.1007/s00348-013-1504-8>

- [12] T. F. Geyer, “Experimental evaluation of cylinder vortex shedding noise reduction using porous material,” *Exp. Fluids*, vol. 61, no. 7, p. 153, Jul. 2020. <https://doi.org/10.1007/s00348-020-02972-0>
- [13] L. Keirsbulck, M. E. Hassan, M. Lippert, and L. Labraga, “Control of cavity tones using a spanwise cylinder,” *Can. J. Phys.*, vol. 86, no. 12, pp. 1355–1365, Dec. 2008. <https://doi.org/10.1139/p08-086>
- [14] M. El Hassan and L. Keirsbulck, “Passive control of deep cavity shear layer flow at subsonic speed,” *Can. J. Phys.*, vol. 95, no. 10, pp. 894–899, Oct. 2017. <https://doi.org/10.1139/cjp-2016-0822>
- [15] F. S. Alvi, C. Shih, R. Elavarasan, G. Garg, and A. Krothapalli, “Control of Supersonic Impinging Jet Flows Using Supersonic Microjets,” *AIAA J.*, vol. 41, no. 7, pp. 1347–1355, Jul. 2003. <https://doi.org/10.2514/2.2080>
- [16] J. J. Choi, A. M. Annaswamy, H. Lou, and F. S. Alvi, “Active control of supersonic impingement tones using steady and pulsed microjets,” *Exp. Fluids*, vol. 41, no. 6, pp. 841–855, Nov. 2006. <https://doi.org/10.1007/s00348-006-0189-7>
- [17] V. F. Kopiev *et al.*, “Jet noise control using the dielectric barrier discharge plasma actuators,” *Acoust. Phys.*, vol. 58, no. 4, pp. 434–441, Jul. 2012. <https://doi.org/10.1134/S1063771012040100>
- [18] M. Alkheir, H. H. Assoum, N. E. Afyouni, K. Abed Meraim, A. Sakout, and M. El Hassan, “Combined Stereoscopic Particle Image Velocimetry Measurements in a Single Plane for an Impinging Jet around a Thin Control Rod,” *Fluids*, vol. 6, no. 12, p. 430, Nov. 2021. <https://doi.org/10.3390/fluids6120430>
- [19] P. Miron, J. Vétel, A. Garon, M. Delfour, and M. E. Hassan, “Anisotropic mesh adaptation on Lagrangian Coherent Structures,” *J. Comput. Phys.*, vol. 231, no. 19, pp. 6419–6437, Aug. 2012. <https://doi.org/10.1016/j.jcp.2012.06.015>